Figure S1. IHC of a human liver tissue microarray. Typical images of liver sections in an array stained with the XC246 antibody (Fig. 1A) and their H&E staining images are presented. The H&E stained images of individual tissues included in this array were provided on the supplier's website (https://www.biomax.us/tissue-arrays/Liver/LV1201b). IHC, immunohistochemistry; H&E, hematoxylin and eosin.

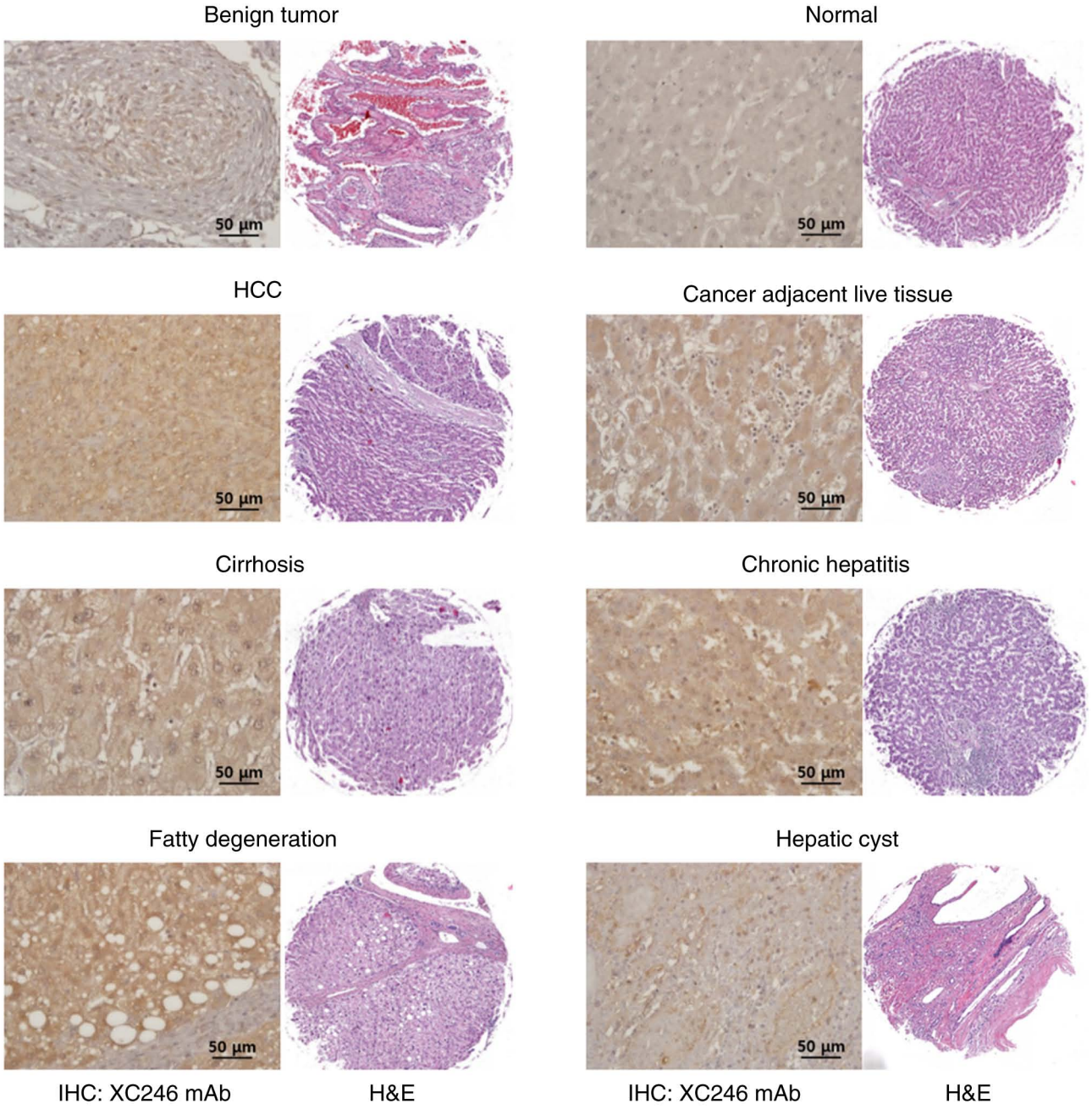

Figure S2. Two-dimensional western blot analysis of the XC246 antigen in HepG2 human liver cancer cells with the XC246 autoantibody. HepG2 cell lysate (760 μg) was separated in the first dimension by isoelectric focusing (pH 3-10) and in the second dimension by 10% SDS-PAGE. The separated proteins were transferred to PVDF membranes, and western blotting was performed with the XC246 autoantibody. To confirm the molecular weight of protein bands detected by immunostaining with XC246 antibody, the images of gel slices loaded with pre-stained molecular markers were placed adjacent to the immunostained blot images. The arrows indicate the proteins reactive in the western blots that correspond to the XC246 protein. The XC246 antigen demonstrated a molecular weight of about 110 kDa and an pI of ~9. SDS-PAGE, sodium dodecyl sulfate-polyacrylamide gel electrophoresis; PVDF, polyvinylidene fluoride; pI, isoelectric point.

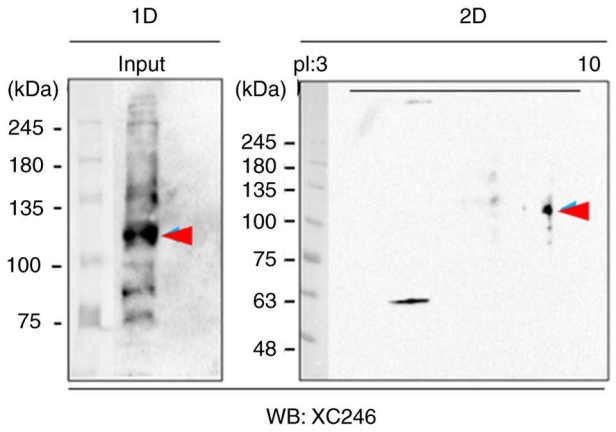

Figure S3. Kaplan-Meier analysis of the overall survival of patients with hepatocellular carcinoma according to their BRD2 protein expression levels using the Human Protein Atlas database (https://www.proteinatlas.org/ENSG00000204256-BRD2/pathology/liver+cancer#imid_11284451). BRD2, bromodomain-containing protein 2.

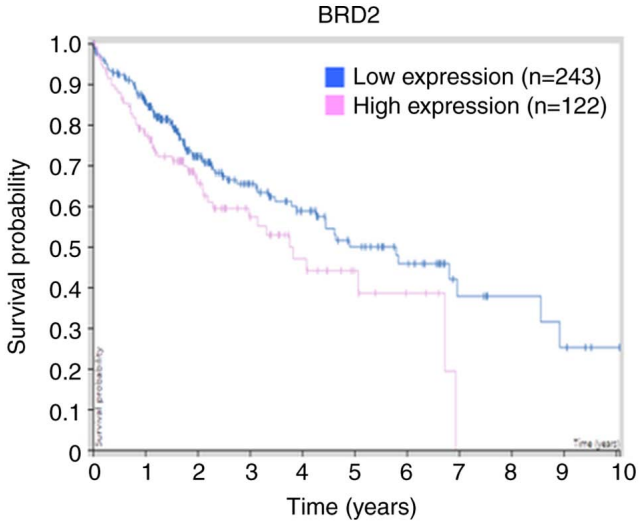

Figure S4. Sequence alignment of the mouse and human BRD2. BRD2, bromodomain-containing protein 2.

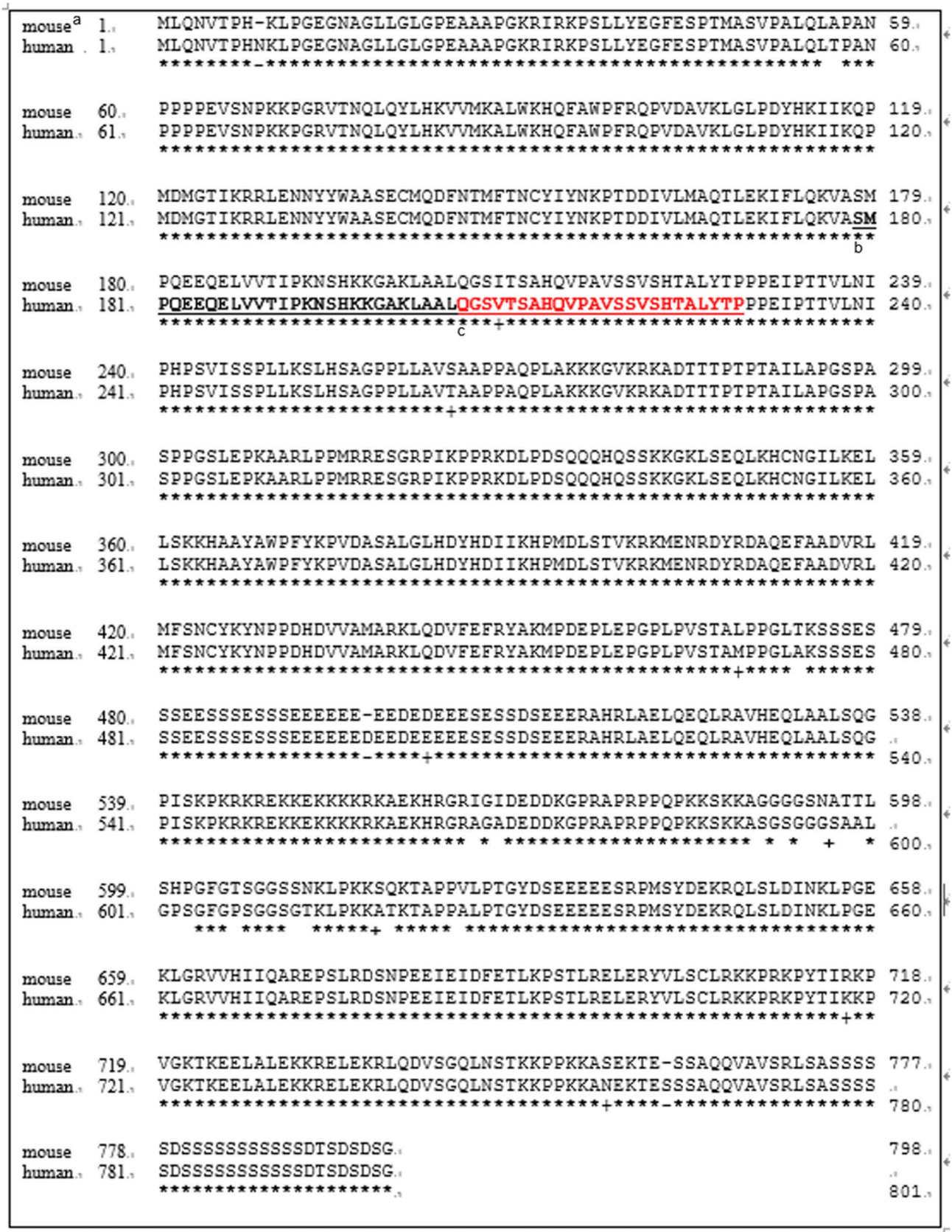

[a]Mouse BRD2 (NP_001191902.1) Length: 798; human BRD2 (NP_005095.1) Length: 801; Identities: 772/801(96%), Positives (+): 780/801(97%), Gaps (–): 3/801(0%).,

[b]BRD2 antibody epitope: human BRD2 (179–205 amino acid residues): bold black text underlined..,

[c]XC246 autoantibody epitope: human BRD2 (206–229 amino acid residues): bold red text underlined.

Figure S5. Validation of subcellular fractionation using specific markers. Equal amount of subcellular fraction lysate (30 μg) was separated by using 10% SDS-PAGE and western blotting, analyzed using anti-ALIX antibody (exosome marker) and anti-calnexin antibody (Cytoplasm or endoplasmic reticulum marker). Tot, total lysate; Cyt, cytoplasmic fraction; Nuc, nuclear fraction; Exo, exosome; ALIX, programmed cell death 6-interacting protein.

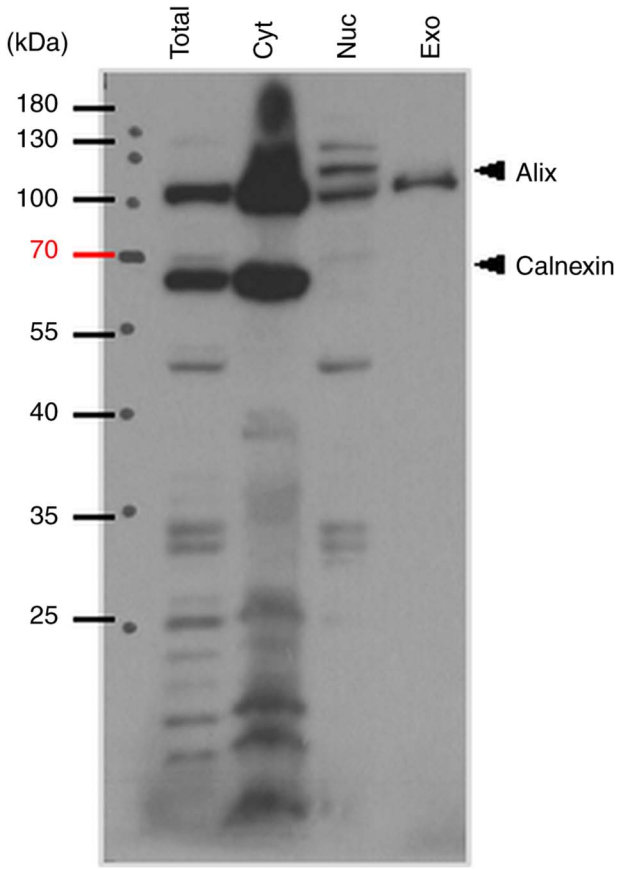

Figure S6. Epitope mapping of the XC246 autoantibody on the human BRD2 protein. Full-length and a series of truncated BRD2 proteins (hBRD2: NM_005104.4), with N-terminal 3X FLAG-tag [(DYKDDDDK)x3], were cloned into the pE28a(+) vector using *Nde*I and *Xho*I. Expression vectors were transformed into *E. coli* strain SHuffle® T7 and cells were cultured for 22 h at 25°C with IPTG. (A) Cell pellets were solubilized in 5X SDS-PAGE buffer and analyzed by Western blotting. Blots were probed with anti-FLAG antibody, XC246 autoantibody, or BRD2 antibodies. Two different BRD2 antibodies (NBP1-84310 or NBP1-30475) were used, which were generated against two different antigenic sites as indicated in panel A. (B) Schematic presentation of a series of BRD2 antigens and their reactivity to antibodies. The epitope of the XC246 autoantibody was defined as residues 206-229 of BRD2. BRD2, bromodomain-containing protein 2; IPTG, isopropyl β-D-1-thiogalactopyranoside; SDS-PAGE, sodium dodecyl sulfate-polyacrylamide gel electrophoresis.

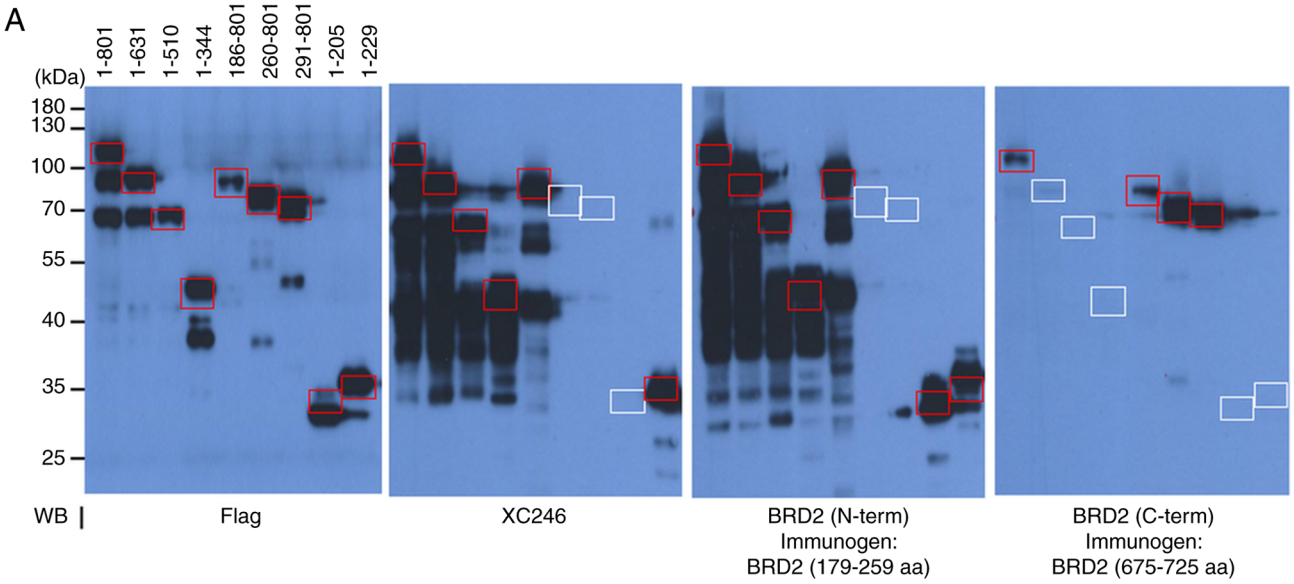

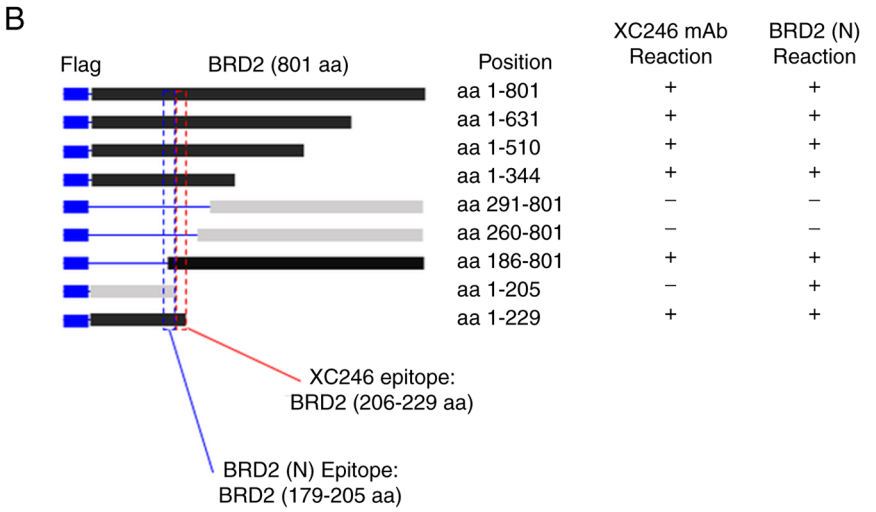

Figure S7. Loss of autoantibody-specific binding to the peptide mimotopes by linearizing the cyclic conformations. The phage-display mimotope peptides, either reduced (linear) or non-reduced (cyclic), were tested for their reactivity to the XC246 autoantibody. For the reduction of the disulfide bond of the cyclic peptides, the epitope-display M13 phages were treated with the reducing reagent, DTT, and iodoacetamide and used as coating antigens (17).

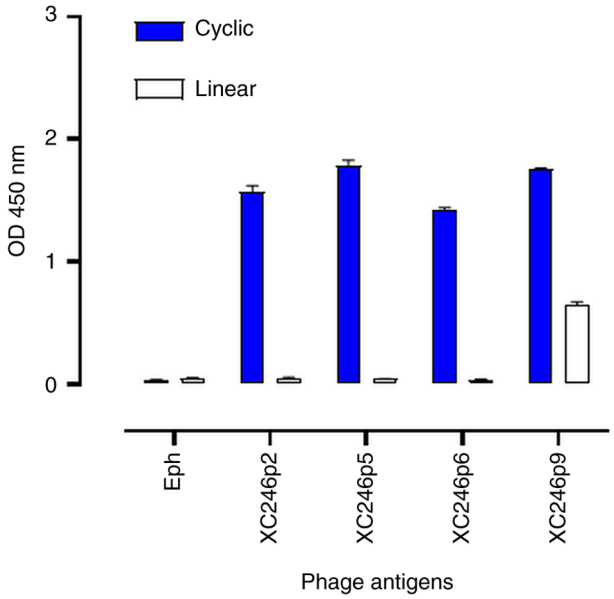

Figure S8. ELISA with BSA-miniPEG2. The indicated amounts of the antigen BSA-miniPEG2 were coated and detected with a gradually diluted XC246 autoantibody. This result is a negative control for the BSA-miniPEG2-XC246p9 ELISA shown in Fig 3E. BSA, bovine serum albumin; ELISA, enzyme-linked immunosorbent assay.

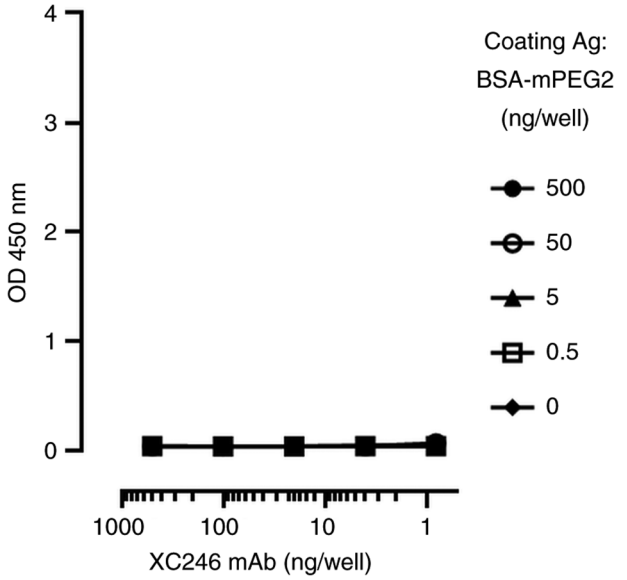

Figure S9. Serum ATIC autoantibody ELISA using XC154p1 mimotope-conjugated BSA. (A) ATIC autoantibody ELISA using BSA-miniPEG2-XC154p1 in sera of patients with HCC as well as non-tumor subjects. Normal (n=91), HCC (n=118), cirrhosis (n=32) and benign liver cancer (n=3) samples. The specific binding of the serum autoantibody to the XC154p1 epitope (anti-ATIC response) was described as the difference in OD between the ELISA for BSA-miniPEG2-XC154p1 and that for BSA-miniPEG2. The CV of the ATIC autoantibody was 0.6125 (RU). (B) The ROC curve analysis displays the diagnostic sensitivity and specificity of ATIC autoantibody biomarker. The clinicopathological features are described in detail in Table III. All experiments were performed in duplicate and repeated a least three times. ATIC, AICAR transformylase/inosine monophosphate cyclohydrolase; BSA, bovine serum albumin; HCC, hepatocellular carcinoma; CV, cut-off value.

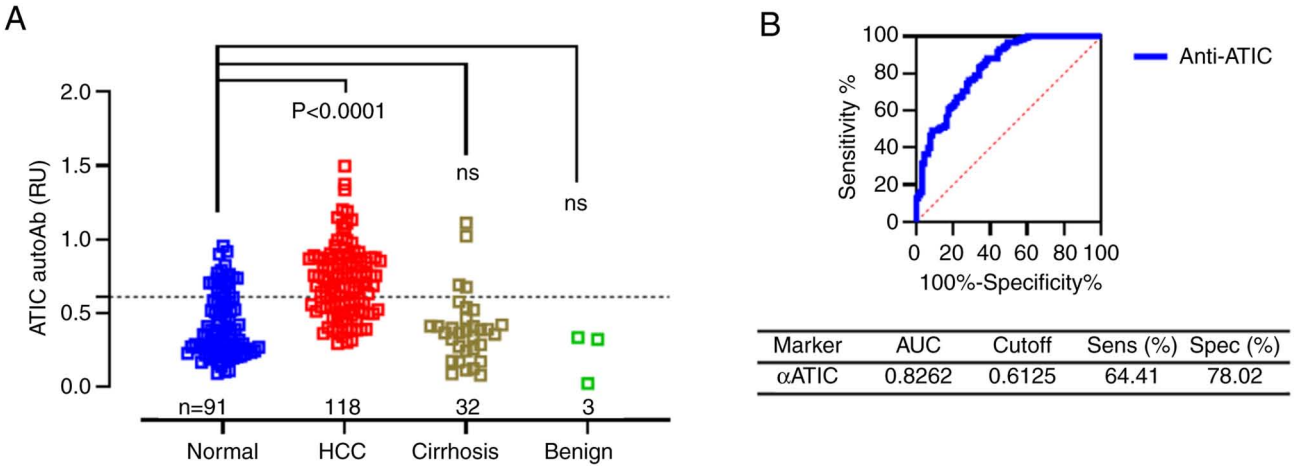

Marker	AUC	Cutoff	Sens (%)	Spec (%)
αATIC	0.8262	0.6125	64.41	78.02

Figure S10. Pearson's analysis of the correlations between the BRD2 autoantibody biomarker and the AFP (A) or ATIC autoantibody (B) in sera of HCC or related disease cohorts. The dotted lines represent the CV of each biomarker diagnosis. BRD2, bromodomain-containing protein 2; AFP, alpha-fetoprotein; ATIC, AICAR transformylase/inosine monophosphate cyclohydrolase; HCC, hepatocellular carcinoma; CV, cut-off value.